
Implication of using auxiliary service voltage transformer sub-stations for rural electrification

Michael Juma Saulo^{1,*}, Charles Trevor Gaunt²

¹Electrical Department. Technical University of Mombasa, Mombasa, Kenya

²Electrical Department. University of Cape Town, Cape Town, South Africa

Email address:

michaelsaulo@yahoo.com (M. J. Saulo), ctgaunt@uct.ac.ke (C. T. Gaunt)

To cite this article:

Michael Juma Saulo, Charles Trevor Gaunt. Implication of Using Auxiliary Service Voltage Transformer Sub-Stations for Rural Electrification. *International Journal of Energy and Power Engineering*. Special Issue: Electrical Power Systems Operation and Planning.

Vol. 4, No. 2-1, 2015, pp. 1-11. doi: 10.11648/j.ijjepe.s.2015040201.11

Abstract: Providing an affordable and reliable electricity supply to rural communities is seen by countries round the world as one of the major keys to development. A good quality and stable electricity supply can provide a wide variety of benefits including lighting (allowing evening activities), clean cooking and heating, access to television/radio, telephone (including mobile), improved health (due to example refrigeration), and many small industrial uses. Often this can be provided by extending the main electricity network to the community. However, for remote rural areas the costs involved can be very high. Therefore, Un-conventional Rural Electrification (URE) technologies are thus very relevant, particularly for countries in sub-Saharan Africa (SSA), as they have potential to make connection to the electricity network affordable. While such systems are already in use, their penetration level is very low. Hence, if the penetration level of such system in power network increases, what is the effect on power and voltage quality, stability and capacity constraints of the overall system? What are the limiting factors, and how can this limit be determined for any particular rural electrification project. These are some of the major questions that this paper address progressively. The paper investigated the maximum penetration level of sub-station based Auxiliary Service Voltage Transformer (ASVT) technologies in transmission power networks with regard to voltage quality, stability, and capacity constraints. This was done by comparing the simulation results of ASVT(s) penetration on a transmission power network with the constructed Surge Impedance Loading (SIL) curves. The curves were derived from the ABCD parameters of the transmission line under investigation. Results showed that ASVT sub-station technologies can be applicable to any HV transmission line whose voltage level is within the 6% tolerance when the load power factor is varied between 0.2 and unity power factor. Moreover, the Loadability tests carried out showed that ASVT system could be operated within allowable voltage profile, if 1MW at 0.3 to 0.5 power factor lagging load was connected.

Keywords: Auxiliary Service Voltage Transformers (ASVTs), Maximum Penetration Level, Sub-Saharan Africa, Loadability Test, ABCD Parameters, Surge Impedance Loading

1. Introduction

In most SSA rural areas, the concentration of electricity users is low and the cost of deploying a conventional sub-station is prohibitive. As a result, in many cases power utilities will not be able to generate an adequate return on the large investment necessary to bring a conventional distribution sub-station on line. On the other hand, there are large numbers of rural communities in these areas living around or in close proximity to high voltage transmissions lines but are un-electrified. The main obstacle is that these lines are carrying high voltages that cannot be directly and

cheaply used for electrification. Therefore, in order to address the drawbacks associated with prohibitive costs of conventional sub-stations, un-conventional auxiliary service voltage transformers (ASVT) sub-station are explored in this paper [1][2].

The ASVT or sometimes known as a station service voltage transformer (SSVT) is insulated in SF6 gas and combines the characteristics of an instrument voltage transformer with power distribution capability [2]. The transformer has power capability of up to about 50kVA to 1MVA for both single and three phase supply. In this transformer the high voltage side is connected directly to the overhead transmission lines. While,

typical secondary voltage ratings are 115V, 230V, 240V, 277V, 480V, and 600 volts. Other voltage level supplies can be designed on order. The system was originally designed to suit supply for auxiliary services within the sub-station such as lighting loads, motor loads and instrumentation purposes [3] [4]. In developing countries where transmission line infrastructure is already in place but a wide-spread distribution infrastructure is lacking, the un-conventional ASVT sub-station technologies can be used as a compact transformer to greatly reduce the electrification costs for small villages or compounds. The ASVT can either be used with its low voltage

output to directly supply needed power for in-close loads near the transmission right of way, or simply step up the ASVT low voltage output through distribution transformers for a local distribution network. Small sub-stations can be sited specific to the load requirements without a large distribution network. Tapping the high voltage transmission line and connecting an ASVT with a small footprint sub-station will provide affordable, readily-available electricity to many rural dwellers in close proximity to high voltage lines and presently without power [2][4]. Figure 1 and 2, show the single line diagram and the pictorial view of an ASVT respectively.

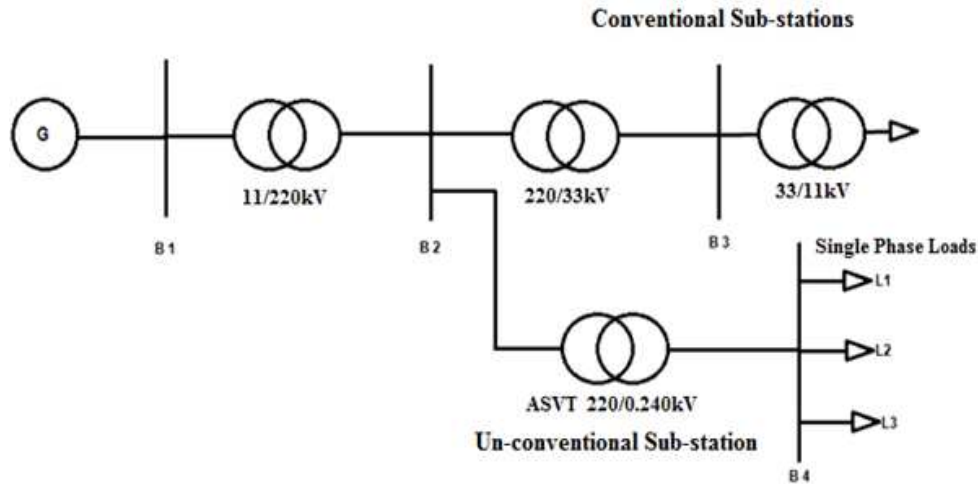


Figure 1. ASVT single line diagram



Figure 2. Auxiliary service voltage transformer (ASVT)

A pilot project was successfully carried out in the rural town of Tubares in Mexico, where ASVTs were used to supply the villagers. The ASVT tapped power from a line of 123kV and transformed it to 230V for distribution purposes. It was reported that a good return on investment was achieved, though not the major objective of this paper. The project brought great developments in the area and has encouraged other rural electrification projects in the region to use the same

technology. According to Gomez et al. [2], the system involves very simple station engineering and presents a successful and economically viable alternative, for electrification of rural communities with load requirements within 50kVA single phase up to 1MVA at three phase arrangement, supplying enough power for applications like refrigeration, water pumping, lighting and other low voltage applications. The use of ASVTs for RE provides the following

benefits [2][8];

- Very high reliable power potential (the number of interruptions in a transmission line are minimum compared with the interruptions usually experienced in a conventional distribution line).
- Solution cost is three times lower than a traditional sub-station. This makes it economically viable for the electrification of rural areas that otherwise would not have opportunity to have the electric service.
- The ASVT is used in a dual function, as a source of power and as an instrument transformer in a single unit, being also used for metering and relaying application.

The main limitation of the system is capacity constraint. Additionally, since the main voltage transforming device of the ASVT is used as a dual function, the failure of one function may lead to the failure of the rest of the system, resulting in power failure to the consumers. Standardization is another barrier with this type of technology. This system has very minimum literature available and this creates curiosity or motivation for investigation. Therefore, the main objective of this paper was to evaluate the implication of using ASVT sub-stations for rural electrification in Kenya. The specific objective was to determine the maximum allowable percentage penetration level of ASVT(s) in power networks with regard to voltage quality, stability, and capacity constraints without steady state voltage violation.

2. Methodology

As mentioned above the specific objective of this paper was to determine the maximum allowable percentage penetration level of ASVTs in power networks with regard to voltage quality, stability, and capacity constraints without steady state voltage violation. This objective was achieved by first designing an ASVT using the reverse design approach developed in section 2.1. System energisation at no-load and load on/off were carried out. Simulations were first done with the line not loaded followed by a loaded line and finally the line under short circuit conditions. Voltage and power variable constraints were taken into considerations. The ASVT units were included at different distances as shown in section 2.2. The line was cascaded with PI sections to increase the speed of convergence and reduce delays in the MATLAB Sim Power software used. Finally, the percentage penetration level of ASVT units in a power transmission network was evaluated based on Surge Impedance Loading (SIL) level of the transmission line under study. The line parameters of this line were first determined using the method described in section 2.2 founded on the ABCD parameter determination [6]. The SIL curve was constructed based on these parameters and compared to the simulation results presented in section 2.3. This comparison was used in section 3.1 to estimate the maximum penetration level of ASVT(s) in the power network. This was done established on the voltage quality and stability constraints.

2.1. Modeling of ASVTs

The developments of transformer design tools and their electromagnetic field for finite elements as well as networks modeling programs allowed the transformers manufacturers to develop the ASVT which can transform high voltage energy from upto 420kV to (below 600V) in one step. ASVTs have high reliability and enough power to fulfill most of the low voltage load application, like control system, pump motors, instrumentation and illumination [2]. To develop an ASVT model, it is first important to understand the magnetic circuit theory and finite element analysis of conventional transformers. Ideally, a transformer stores no energy- all energy is transferred instantaneously from input to output. In practice, all transformers do store some undesired energy, through the following ways [3][7];

- Leakage inductance, which represents energy stored in the non-magnetic regions between Windings, caused by imperfect flux coupling. In the equivalent electrical circuit, leakage inductance is in series with windings, and the stored energy is proportional to load current squared.
- Mutual inductance (magnetizing inductance), represents energy stored in the finite permeability of the magnetic core and in small gaps where the core halves come together. In the equivalent circuit, mutual inductance appears in parallel with the windings. The energy stored is a function of the volts-second per turn applied to the windings and is independent of load current.

Two models of analysing transformers are considered for the ASVTs design, the first model is based on the magnetic circuit theory and the second is based on magneto-static finite element analysis. In this paper the transformer reverse design method is incorporated for the two models.

2.1.1. Reverse Transformer Design

In the conventional method of transformer design, the terminal voltages, VA rating and frequency are specified. In the reverse design approach the physical characteristics and dimensions of the windings and core are the specifications. By manipulating the amount and type of material actually to be used in the transformer construction, its performance can be determined. This is essentially the opposite of the conventional transformer design. It allows for customized design, as there is considerable flexibility in meeting the performance required for a particular application. This type of design is suitable for ASVT models since they are meant for customized application [7][9]. In the reverse design method, the transformer is built up from the core outwards. The core cross section dimensions (diameter for a circular core and side lengths for a rectangular core) are selected from catalogues of available materials. A core length is chosen. Laminations that are available can be specified in thickness. A core stacking factor can be estimated from the ratio of iron to total volume. Figure 3, shows a transformer profile of known material characteristics and dimensions [10].

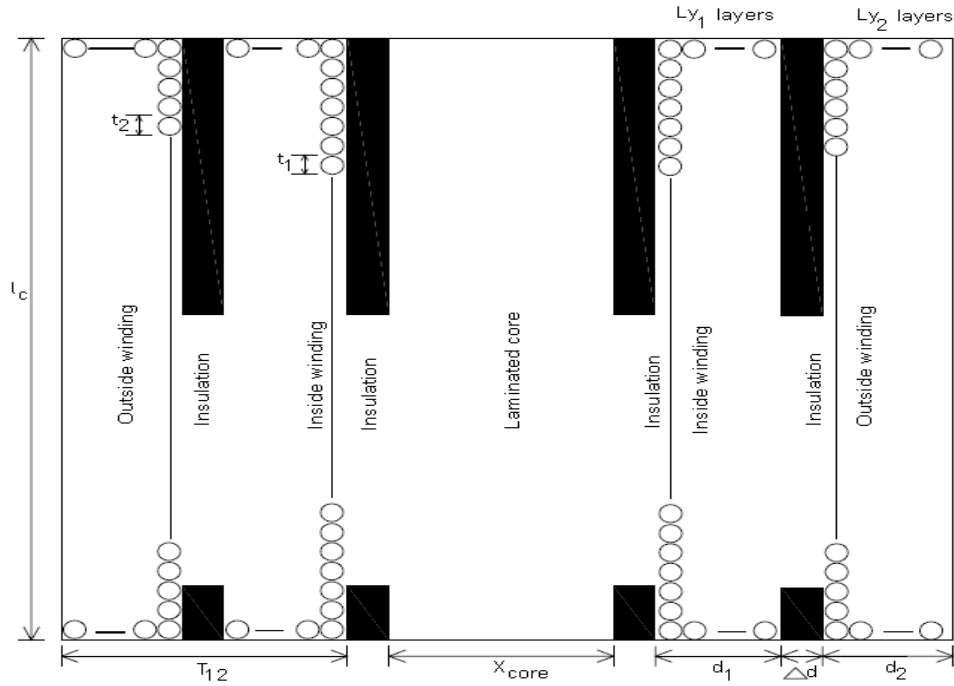


Figure 3. Component dimension and material properties of a transformer

Given the core length l_c and diameter, (or b_{core} and w_{core} for a rectangular core), the inside winding usually low voltage winding is wound on layer by layer. The wire size can be collected from catalogues. Insulation thickness is also specified. The designer can then specify how many layers of each winding are wound. Insulation is placed between core and the inside winding (fomer) and between each layer for high voltage applications. The outer winding usually the HV windings is wound over the inside winding, with the insulation between layers according to the voltage between them. Windings current densities and volt per turn become a consequence of the design, rather than a design specification. The only rating requirements are the primary voltage and frequency. The secondary voltage and transformer VA rating are a consequence of the construction of a transformer.

The number of turns are estimated to be ;

$$N_1 = \frac{l_c L_1}{t_1}, N_2 = \frac{l_c L_2}{t_2} \quad (1)$$

Where;

l_c is the length of core

L_1, L_2 Number of primary and secondary winding layers

t_1, t_2 axial thickness of primary and secondary wire

This calculation assumes that the winding length is equal to the core length. The actual winding lengths may be used if the primary and the secondary winding lengths are different and do not fully occupy the winding window height.

2.1.2. Equivalent Circuit Models

The Steinmetz 'exact' transformer equivalent circuit shown in Figure 4 is used to represent the transformer at supply frequency. Each component of the equivalent circuit can be calculated from the transformer material characteristics and dimensions [9][11].

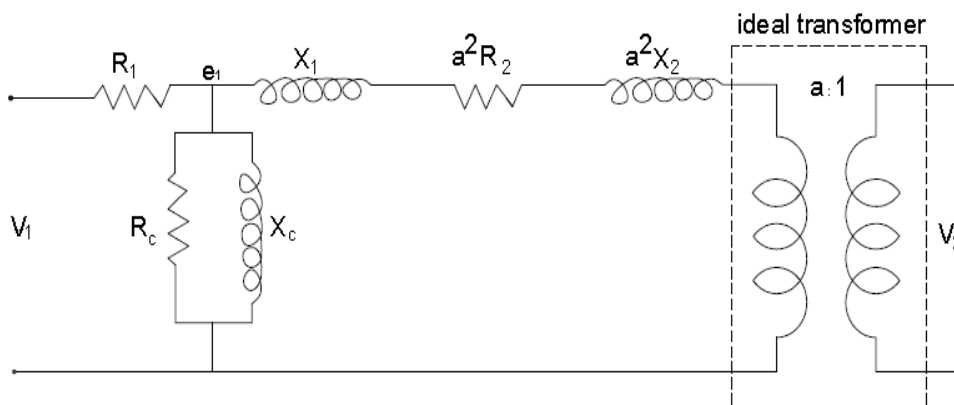


Figure 4. Steinmetz 'exact' transformer equivalent circuit

Based on the equivalent circuit model shown in Figure 4 different aspect of resistance models can be calculated or analysed.

2.1.3. Core Loss Resistance

The losses in the core consist of two major components, the hysteresis loss and the eddy current loss. The hysteresis loss can be calculated using [11].

$$P_k = k_h f B^x WT \quad (2)$$

Where: k_h = Constant depending on the material typically 0.11.

x = Steinmetz factor, typically 1.85

WT = Weight of the core.

B = Peak flux density, calculated from the transformer equation

$$V_i = 4.44 f N_1 \phi \quad (\phi = B A_c)$$

The eddy current is expressed as

$$P_{ec} = \frac{c_l^2}{12 p_c} \frac{l_c}{N_1^2 A_c} e_1^2 k_v \quad (3)$$

Where:

c_l = lamination thickness

p_c = Operating resistivity of the core

A_c = cross-sectional area of the core

e_1 = induced primary winding voltage

k_v = total core volume/central limb volume

The variation of resistivity with temperature should be accounted for, since the transformer will be heated up under operation. The operating resistivity for a material at temperature $T^{\circ}C$ is,

$$\rho = \rho_{20^{\circ}C} (1 + \Delta\rho(T - 20)) \quad (4)$$

Where: $\Delta\rho$ = thermal resistivity coefficient

$\rho_{20^{\circ}C}$ = material resistivity at $20^{\circ}C$

The hysteresis and eddy current losses can be expressed in terms of induced voltage e_l ,

$$p_h = \frac{e_l^2}{R_h}, p_{ec} = \frac{e_l^2}{R_{ec}} \quad (5)$$

Where, R_h = hysteresis loss equivalent resistance

R_{ec} = eddy current loss equivalent resistance

Thus, both R_h and R_{ec} can be included in the model as the core loss resistance R_c , calculated as,

$$R_c = \frac{R_h R_{ec}}{R_h + R_{ec}} \quad (6)$$

2.1.4. Inductive Reactance Models

Magnetizing reactance is given by [10],

$$X_m = \frac{\omega N_1 \mu_0 \mu_{rc} A_c}{I_{eff}} \quad (7)$$

Where; $\omega = 2\pi f$

μ_0 = Permeability of free space ($4\pi \times 10^{-7}$ H/m)

μ_{rc} = Relative permeability of core.

I_{eff} = effective path length for mutual flux.

2.1.5. Leakage Reactances

The primary and secondary leakage reactances are assumed to be the same, when referred to the primary, and are each half of the total transformer leakage reactance. One form of the expression is [10],

$$X_1 = a^2 X_2 = \frac{1}{2} \frac{\mu_0 N_1^2}{l_c} \left(\frac{l_p d_1 + l_s d_2}{3} \right) + l_{ps} \Delta d \quad (8)$$

Where; l_p, l_s = mean circumferential length of primary and secondary windings.

l_{ps} = mean Circumferential length of interwinding space.

d_1, d_2 = Thickness of primary and secondary windings

Δd = Thickness of interwinding space.

Having obtained the component values, the equivalent circuit can be solved. Open circuit, short circuit and loaded circuit performances can be estimated by putting an impedance $Z_L = R_L + jX_L$ across the output and varying its value. Consequently, performance measure of voltage regulation and power transfer efficiency for any load condition can be readily calculated. Current flows and densities in the windings can be calculated and compared to desired levels. The next section shows the detail design of the ASVT system.

2.1.6. ASVT Design

Figure 5, illustrates the ASVT design flow chart, the process is initialized by setting up the technical specifications, of the transformer to be designed, using the power rating of the transformer as captured in the technical specification, secondary volt/turn is determined. This secondary volt/turn is then used to determine the secondary turns. By use of the secondary/primary voltage ratio, the primary turns are determined. The primary and secondary turns are then used to determine the transformation ratio. The calculated turns ratio is then compared with the turns ratio in the technical specifications, if not the processor transfers control to start off the process, if yes, the central processing unit proceeds to determine the core area then the core diameter, core stack, step width, number of coils per turn, weight of the core, conductor diameter and number of coils per turn [12][13].

The system is then constructed, operational test and current

leakage test administered. If the required parameters have not been achieved the process is repeated. If the system operates as expected, the process is finished and the system dispatched.

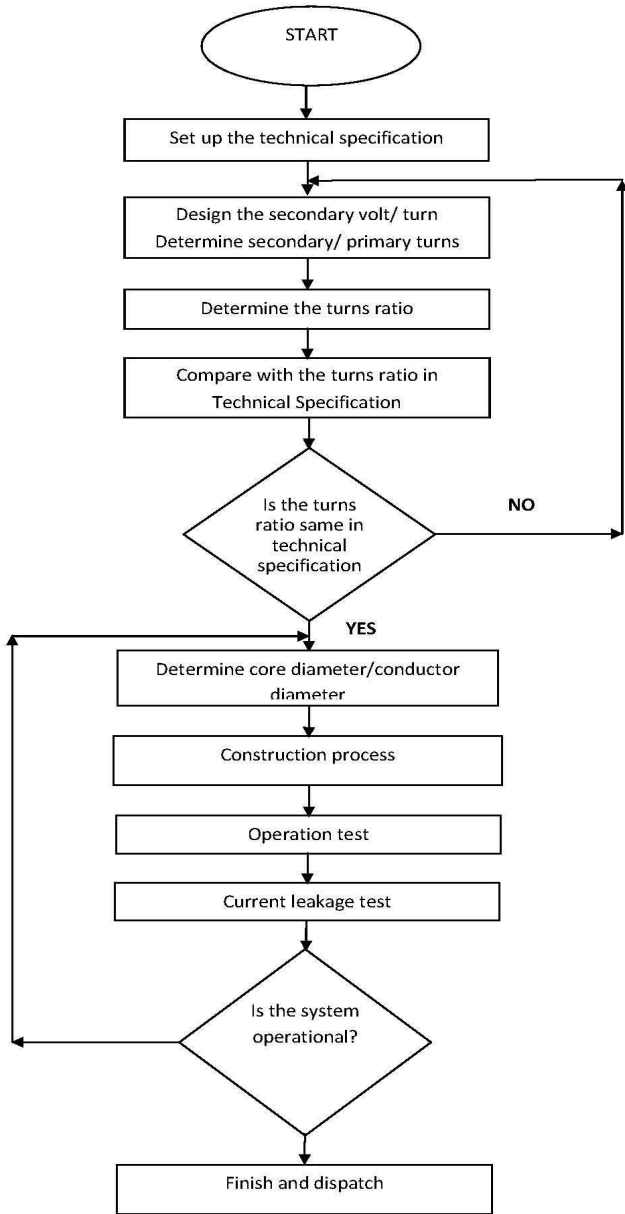


Figure 5. Flow Chart for Asvt Design

2.2. Determination of Transmission Line Parameters

Before surge impedance loading curves can be constructed it was important to determine the transmission line parameters. The method used was based on synchronised phasor measurements [6] This method uses the two-port ABCD parameters that is defined in [8]. The ABCD parameters give the relationship between the voltages and currents at two points. For a transmission line this means that the ABCD parameters represents the influence that the capacitance, inductance and resistance of the line has on the voltage and current values measured at the sending and receiving end sides. The relationship is given by the

following equations.

$$\begin{bmatrix} V_s \\ I_s \end{bmatrix} = \begin{bmatrix} AB \\ CD \end{bmatrix} \begin{bmatrix} V_r \\ I_r \end{bmatrix} \tag{9}$$

A and B are defined by the following equations.

$$A = \cosh \gamma l \tag{10}$$

$$B = Z_c \sinh \gamma l \tag{11}$$

Where

$$Z_c = \sqrt{\frac{z}{y}} \tag{12}$$

From the preceding equation it is seen that once A and B are known, z and y can be calculated. Therefore, z and y have been defined as the series impedance and shunt admittance per unit length. In order to solve for A and B two operating points that are linearly independent have to be considered. A matrix can be constructed for the measurements of the two cases.

$$\begin{bmatrix} V_{s1} \\ V_{s2} \end{bmatrix} = \begin{bmatrix} V_r 1 I_r 1 \\ V_r 2 I_r 2 \end{bmatrix} \begin{bmatrix} A \\ B \end{bmatrix} \tag{13}$$

Using Cramer’s Rule A and B can be calculated.

$$A = \frac{\det \begin{bmatrix} V_{s1} I_r 1 \\ V_{s2} I_r 2 \end{bmatrix}}{\det \begin{bmatrix} V_r 1 I_r 1 \\ V_r 2 I_r 2 \end{bmatrix}} \tag{14}$$

$$B = \frac{\det \begin{bmatrix} V_r 1 V_s 1 \\ V_r 2 V_s 2 \end{bmatrix}}{\det \begin{bmatrix} V_r 1 I_r 1 \\ V_r 2 I_r 2 \end{bmatrix}} \tag{15}$$

To calculate y and z the results from (14) and (15) are substituted into (10) and (11) while Z_c substituted with equation (12) and $\gamma l = \sqrt{yz}l$

This provides two equations with two unknown to solve. The method was very useful since the impedance was given as a value with an angle. This meant that the resistance and inductance were given as separate values. This was also the only method that gave the shunt admittance (y) from where the capacitance can be calculated. This method was used in section 3.1 to help in constructing the SIL curve.

2.3. ASVT Loadability

Loadability tests were also carried out to show the variation of load voltage with load MVA. The main issue of the loadability test was to find the optimum operating load MVA that can be supported before the voltage begins to

collapse. The tests were done at variable power factor. Figure.6 below shows the model of the ASVT loadability test system used while Figure 7 is the loadability test graph. The load model used was that of series R-L. The system was tested in six different levels of demand. For each test, real

power (P_L) was fixed and reactive power (Q_L) varied to operate at different load power factor between 0.2 lagging to unity. Simulation results are as shown in Figure 5. Acceptable voltage drop at the load terminal was $\pm 6\%$ of 12.7kV.

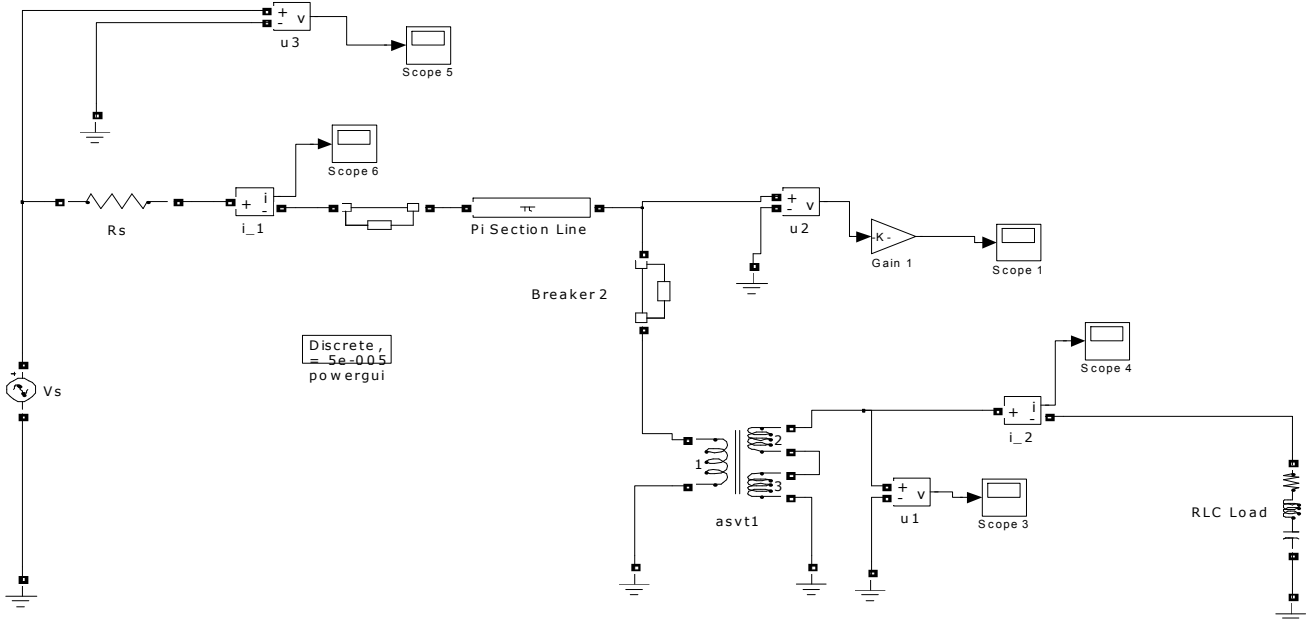


Figure 6. ASVT Loadability Model

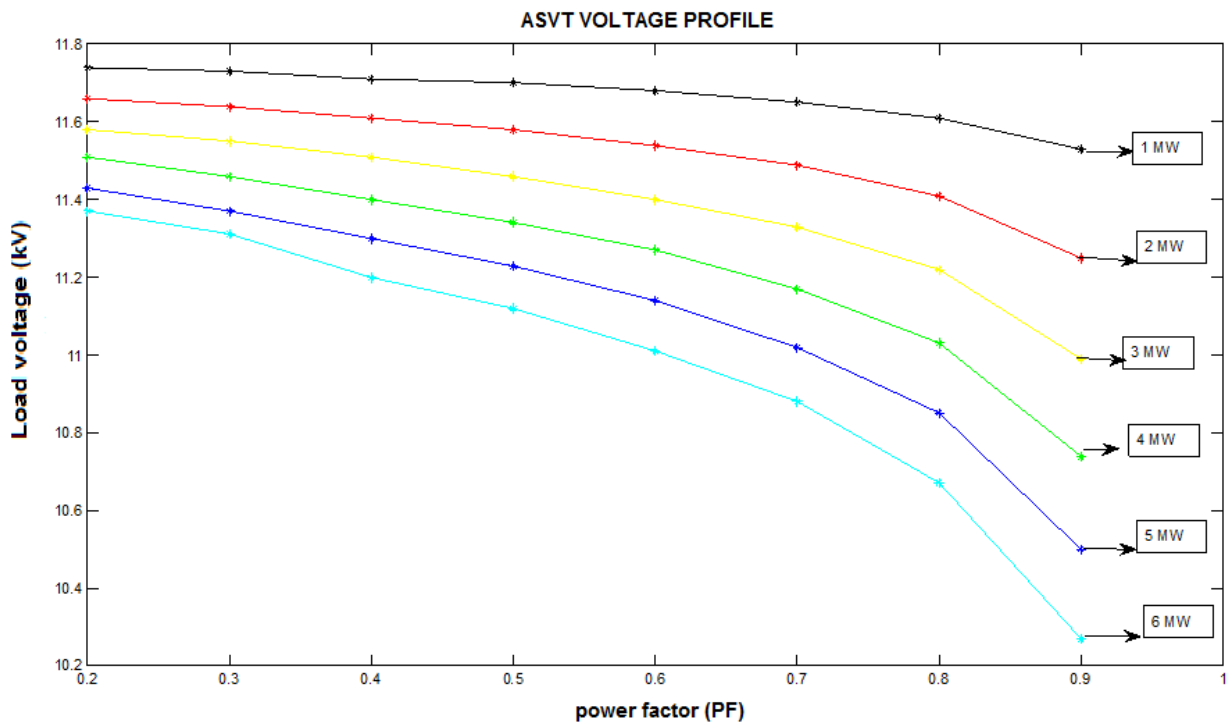


Figure 7. Loadability test of ASVT

Simulation results clearly showed that ASVT system can be operated within allowable voltage regulation if a load of 1MW at 0.3 to 0.5 power factor was connected at the load terminal. The current at these power factors ranged between 60.07A to 63.27A. These currents were slightly higher due to

the poor power factor. It was worth noting that the 6MW load had an unacceptable load profile voltage profile between 0.2 and 0.9 power factors. Although, the load currents were quite high i.e. between 110.74A and 226.14A.

3. Results and Analysis

3.1. Determination of the SIL Curve

The final test was to determine whether it would be possible to draw a SIL curve from the measured data derived in section 2.2 across a transmission line. The model that was used to determine the feasibility of the SIL curve is shown in Figure 8.

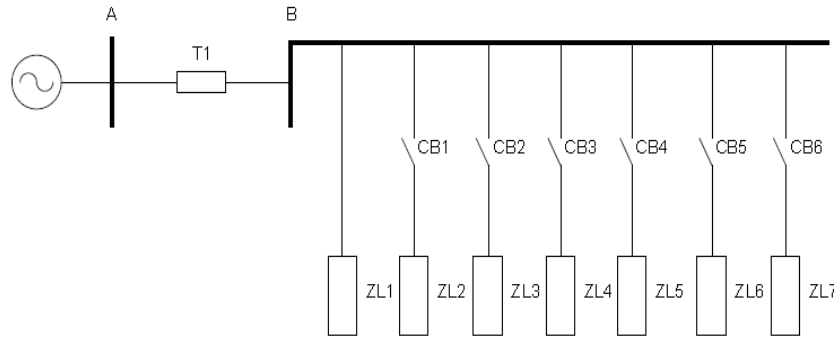


Figure 8. Simulation circuit used for drawing the sil curve

For this part of the simulation three SIL curves were constructed under three distinct operating conditions for comparison with the loadability test in section 2.3. For the first and second conditions the loads had a power factor of 0.5 and 0.9 respectively. The last simulation was done for loads with varied power factors. Table 1 shows the loads that were used. This power factors were chosen based on the results obtained in section 2.3. This was done in order to make the evaluation of loadability and penetration level of ASVTs rational.

Table 1. size of impedance load in conjunction with time

Time (s)	Load (MVA)		
	PF = 0.5	PF = 0.9	Mixed PF
0 – 0.7	2	1.11	1.11
0.7 – 1.4	3	1.66	2.11
1.4 – 2.1	5	2.77	4.11
2.1 – 2.8	6	3.33	4.66
2.8 – 3.5	8	4.44	6.66
3.5 – 4.2	9	4.99	7.66
4.2 – 4.9	11	6.11	8.77

The Figure shows seven loads with six circuit breakers. The circuit breakers were used to switch the selected load across the power line. The simulation was done over a total of 4.9 seconds. The power factor of the load had to be the same for all the seven loads. The reason for this was that the transmission line reacts differently to different amounts of reactive power transferred.

Figure 9 to 11 showed practical SIL curves drawn from measured data. The SIL curves were drawn for different power factors starting from a power factor of 0.5.

In most cases a power factor of 0.5 is uneconomical. The typical values for power factors across a transmission line are in the range of 0.8 to 0.95. The reason for using a power factor of 0.5 was first to compare the results to the one presented in section 2.3. Secondly, to see the difference in the SIL curves between power factors of 0.9 and 0.5. Both power factors are used in Figure 11.

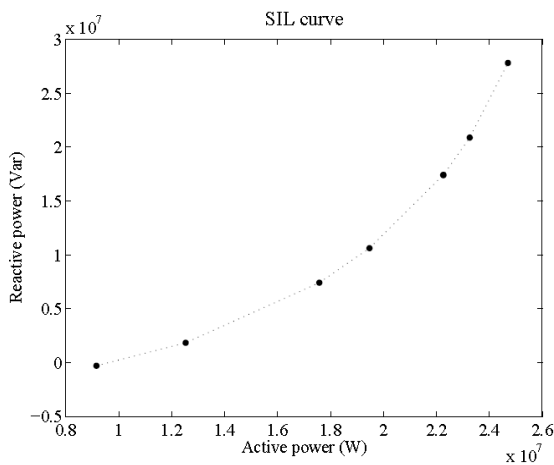


Figure 9. Sil curve with power factor of 0.5

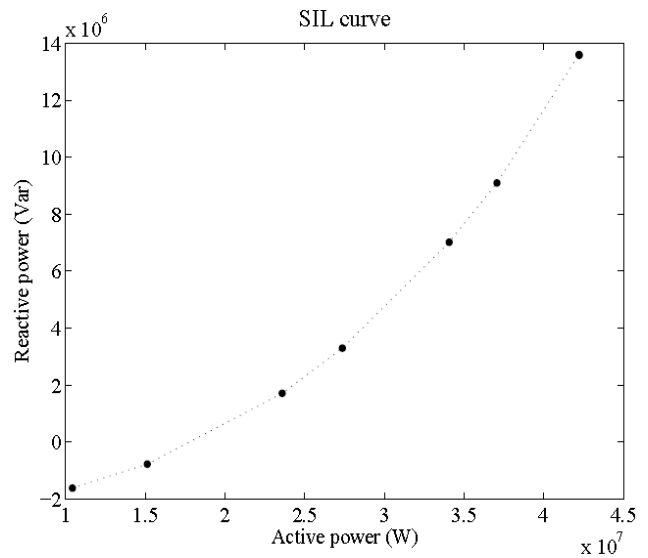


Figure 10. SIL curve with power factor of 0.9

Figure 10, shows the SIL curve constructed for a power factor of 0.9. An individual SIL curve does not have to be drawn for every possible power factor. Rather, a SIL curve must be constructed for power factors within an operating step. It was decided to use a step size of 0.1. In this case there were two SIL curves for the transmission line: one when the power factor ranges between 0.8 and 0.89 and another for the power

factor equal to and larger than 0.9. The decision for the step change was based on the curve of Figure 11. For this SIL curve, the power factors of the loads were switched in varied between 0.5 and 0.9.

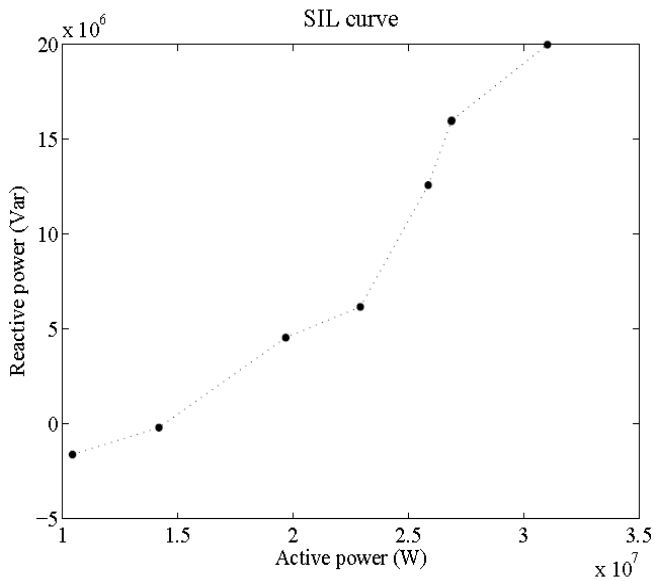


Figure 11. Sil curve with mixed power factors

Simulation results for the SIL curve proved that it is possible to construct the curve from measured data. It is important to note that a different SIL curve had to be drawn for a range of power factors. From Figure 11 it is evident that a mixed power factor will not result in a smooth SIL curve. Even though with the high difference in power factors, the SIL curve still retained its general shape. Thus, we can deduce that a SIL curve will be smooth for a range of power factors. In addition, to the active and reactive power measurements needed for the construction of the SIL curve, the load side power factor has to be determined as well. This power factors were then used to determine the SIL curve to which the measured data can be added.

4. Penetration Level of ASVT in Power Network

Based the parameters of the 220kV, 440km long Kiambere-Rabai under study in this paper. The line was estimated to have an X value of 0.3752pu at a SIL of 124MW. Consequently, with reference to the simulation results shown from Figure 12 to 15. The Penetration results exhibited increased distortion towards the sending end of the line. These distortions of impulses which last between 2 to 3 cycles on switching accumulatively could cause insulation failure on the ASVT and its associated gears connected to the line. However, penetration of two similar ASVTs provided much improved characteristics for both transmission line and output of the sub-station while distortion effect was limited to less than two cycles. This may be attributed to the fact that with higher shunt compensation, it becomes possible to transfer power over long distance without violating the voltage stability or voltage quality limits. With addition of an extra ASVT, no significant change was observed. It would be right to deduce that the designed SIL did not accurately correlated to the line characteristics, but as the numbers of ASVT units were increased the line voltage profile improved as observed from the simulation results. This indicates that when a line is terminated at its SIL the complex power gain (actually loss) is purely real. The implication of this is that the line (when terminated at SIL), only affects the real power (decreases it) but does not affect the reactive power at all. Whatever reactive power flows out of the line (and into the load) also flows into the line. Therefore, a line terminated at SIL has a very special characteristic with respect to reactive power. The amount of reactive power consumed by an ASVT is exactly compensated by the reactive power supplied by the line for every length of the line. Consequently, the maximum penetration level of ASVT units in a power transmission network is governed by their surge impedance loading (SIL).

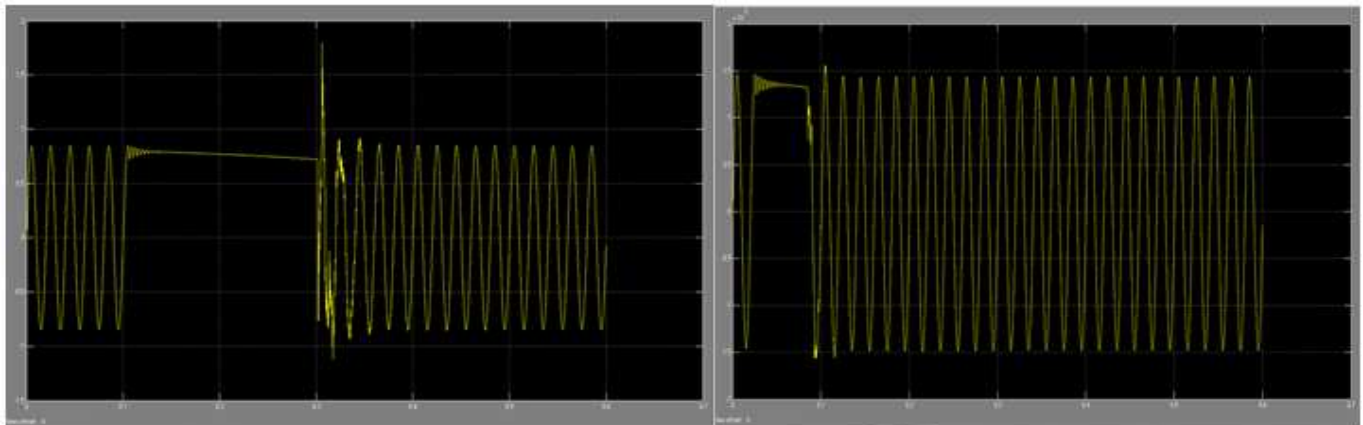


Figure 12. Tap-off voltage and load voltage waveforms for an ASVT.

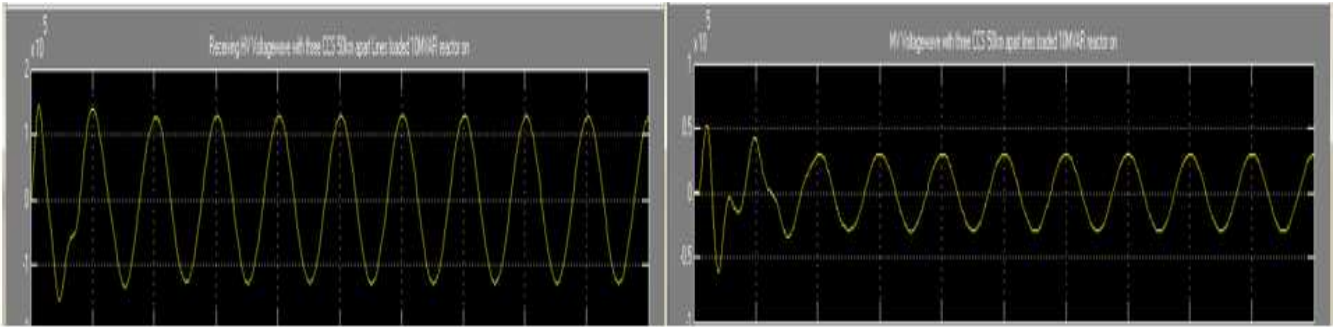


Figure 13. Sending and Receiving end Voltages for three ASVT at different distances

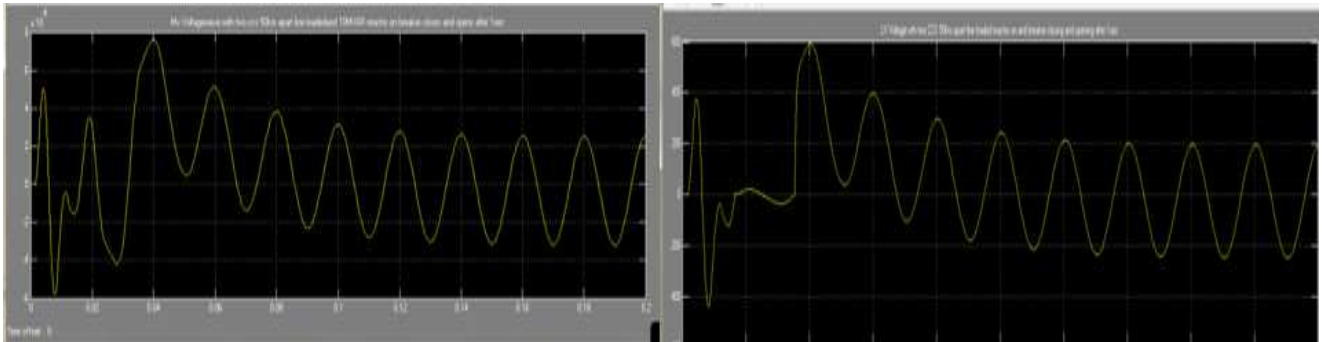


Figure 14. MV and LV Voltage with breaker closing after 1 second

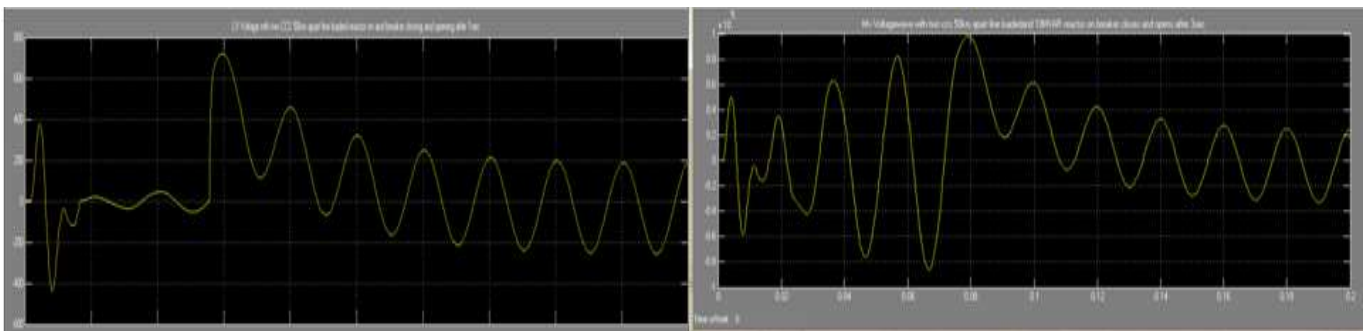


Figure 15. MV and LV Voltage with breaker closing after 2 seconds

5. Conclusion

The transmission network under investigation was a 220kV, 210MW; 440km Kindaruma to Rabai line in Kenya. Considering, an ASVT model rated at 127kV/240V, 100kVA with provision for load tap-changer. Line loadability curves in Figure 5 were used for comparison with the results obtained in section 3.1. Estimates of the power transfer capability value at 50Hz for other different voltages were also determined. For example based on the line parameters determined and the load curve constructed for the 220kV line. The loadability curve at a power factor of 0.5 showed that the reactive power was at 1.732MVAR with a load current and voltage of 60.34A and 11.5kV respectively. Conversely, the results of the 0.5 power factor SIL curve showed that for the same amount of reactive power, an active power of 2.2MW, with a load current of 11.56A may be connected to the system. Hence, the 0.9 power factor loadability curve showed that for a reactive power of 0.484MVAR, the active power was approximately 1.70 MW.

The load current and voltage were 80.02A and 11.6kV respectively. The SIL curve at 0.9 power factor showed that for the same amount of reactive power, an active power of 1.75MW may be connected in the system. The mixed power factor (Figure 9) validated the results. That is, it showed that for the two power factor of 0.5 and 0.9, an active power of about 1.70MW required almost a similar amount of reactive power of about 1.732MVAR. This showed that it was un-economical to operate the ASVT at low power factor (pf = 0.5). At this power factor it was proved that the loadability of the ASVT was quite low. In order to improve the loadability and stability of the system, the line had to be compensated.

Acknowledgements

We want to thank my sponsors The Technical University of Mombasa (TUM) and National Commission for Science and Technology (NACOSTI), for giving me this opportunity to be able to research and publish this paper. Thank you very much for your financial support.

References

- [1] Pasand, M.S., Aghazadeh, R., (2003). Capacitive Voltage Substations Ferro resonance Prevention using power electronics devices International conference on power system transients- IPST 2003 in New Orleans.
- [2] Gomez, R.G., Solano, A.S., Acosta, E.A., (2010): Rural Electrification Project Development, Using Auxilliary Transformers. Location of Tubares, Chihuahua, Mexico. CIGRE C6-305- 2010 working group (Coll 2010) "Rural Electrification" Calgary.
- [3] Artech Instrument transformer manual (2010): ASVT – 245 and ASVT 145 Manuals and technical brochures.
- [4] Saulo, M.J., Gaunt C.T., and Mbogho, M.S., (2012): Comparative Assessment of Capacitor Coupling Sub-station and Auxiliary Service Voltage Transformer for Rural Electrification 2nd annual Kabarak international conference at Kabarak University 16th -18th October 2012 Nakuru, Kenya.
- [5] Barnes, D.F., (2007): The challenge of Rural Electrification: Strategies for developing countries. Vol 3 pp1-18 Washington DC.
- [6] Wilson, R. E., Zevenbergen G. A., Mah, D.L., Murphy, A. J., (1999): Calculation of transmission line parameters from synchronised measurements Taylor and Francis, Vol 27, pp1269-1278, 1999.
- [7] Bell, S.C., Bodgers P.S., (2007) Power Transformer Design Using Magnetic Theory Finite Element Analysis-Comparison of Techniques Proceeding of AUPEC 2007 Perth, Western Australia 9-12 December 2007.
- [8] Grainger J.J., and Stevenson W.D., (1994): Power System Analysis, Singapore: McGraw Hill 1994, pp 141-233.
- [9] Margueron, X., Keradec, J.P., (2007): Design of equivalent circuit and characterization strategy of n-input coupled inductors. IEEE Transactions on Industry Applications Jan-Feb 2007, vol 43, Issue 1, pp14-22
- [10] McLyman, W.N., (2004): Transformer Inductor and Design Handbook, 3rd edition, 2004. Dekker, New York, USA,
- [11] Paul, C.R., Nasar, S. A., Unnewehr, L.E., (1986): Introduction to Electrical Engineering McGraw-Hill, Singapore, 1986.
- [12] Wadhwa, High Power system analysis and applications, The Electricity Authority of New South Wales, Fourth Edition, June 2010.
- [13] Anderson, G.O., Yanev, K., (2010): Non-Conventional Sub-station and Distribution System for Rural Electrification. 3rd IASTED Africa PES 2010, Gaborone, Botswana, September 2010.